

Coordinated Operation of Mobile Emergency Generators and Local Flexible Resources for Distribution Network Resilience Enhancement

Kaiqing Qiu, Wei Gan*, Yue Zhou, Wenlong Ming, Jianzhong Wu

School of Engineering, Cardiff University, Cardiff, UK

GanW4@cardiff.ac.uk

ABSTRACT

The increasing electrification of energy demand and connection of distributed energy resources pose a high burden on electrical power systems. Future power distribution networks are increasingly vulnerable to disruptions and extreme events with less redundancy of network capacity. This paper proposes a novel coordinated operation scheme to improve power distribution network resilience, assessing the value of operating mobile emergency generators (MEG) in coordination with other flexible resources. Three forms of flexibilities are considered in this research: flexibility from networks, local distributed energy resources, and mobile emergency generators. An optimization model is formulated and demonstrated on a European representative distribution network. Results show the value of mobile emergency generators to provide emergency services through coordinating with existing energy networks and distributed energy resources, thereby contributing significantly to power distribution network resilience.

Keywords: Power distribution network, mobile emergency generator, distributed energy resources, resilience improvement.

NONMENCLATURE

Abbreviations

MEG	Mobile emergency generator
LES	Local energy system
DER	Distributed energy resource
PDS	Power distribution network
PV	Photovoltaics

Symbols

K	Set of MEG units
---	------------------

L	Set of distribution lines
N	Set of nodes
T	Set of time intervals
k	Indices of MEG unit
i, j	Indices of nodes
t	Indices of time intervals
C^{voll}	Value of lost load
C^{im}	Electricity import price
C^{trans} / C^{MES}	MEG transport/fuel price
r_{ij} / x_{ij}	Line resistance/reactance
V_t^{min} / V_t^{max}	Lower/upper bounds of nodal voltage square
V_0	Voltage square in the slack node
$P_{i,t}^D$	Rated load demand in each node
$\bar{P}_{i,t}^{im} / \bar{P}_{i,t}^{ex}$	Maximum import/export power
$\bar{P}_{i,t}^{Batt}$	Battery maximum output power
$\bar{P}_{k,i,t}^{MES}$	Maximum MEG output power
$E_{min}^{Batt} / E_{max}^{Batt}$	Minimum/Maximum stage of charge
η	Battery efficiency
T_{trans}	MEG transportation time delay
$P_{i,t}^{ls}$	Load shedding amount
$P_{i,t}^d$	Actual load demand
$P_{k,i,t}^{MES}$	MEG output power
P_t^{ij} / Q_t^{ij}	Branch active/reactive power flows
$P_{i,t}^{im} / Q_{i,t}^{im}$	Net import power in each node
$P_{i,t}^{ex} / Q_{i,t}^{ex}$	Net export power in each node
$P_{i,t}^{ch} / P_{i,t}^{dis}$	Battery storage charge/discharge power
V_i^t	Square of nodal voltage magnitudes
Z_t^{ij}	Distribution line real state
$X_{i,t}^{ch} / X_{i,t}^{dis}$	Battery charge and discharge state

$\lambda_{k,i,t}$	MEG connection state
$u_{k,i,t}$	MEG location state
$\mu_{k,i,t}^{trans}$	MEG transportation state

1. INTRODUCTION

The energy revolution is undergoing on a worldwide basis, featured by the transition from traditional fossil fuels towards low-carbon and renewable energy and the electrification of heat and transport. This poses both challenges and opportunities to the energy systems. From the power system perspective, one key challenge lies in the surging electrical demand, which puts considerable strain on the networks [1]. As a result, network reliability and resilience may be negatively impacted when emergencies are taking place due to the overloading of certain components. Thus, ensuring the resilience of power distribution networks (PDN) by effectively utilizing existing resources and exploring future technical options becomes necessary.

The anticipated reduced redundancy in network capacity of future PDNs increases their vulnerability to potential disruptions or threats. Addressing this problem through upgrading networks requires large upfront costs. Therefore, more non-network solutions are proposed such as promoting distributed energy resources (DERs) at the local level, including rooftop solar photovoltaics (PV), wind turbines, energy storage systems, and other distributed generators (DGs). These locally-built resources facilitate the establishment of local energy systems (LESs) [2], offering several benefits such as cost reduction, peak demand mitigation, and system resilience enhancement.

Another emerging solution for supporting resilient network operation is the deployment of mobile flexible resources, such as mobile emergency generators (MEGs) [3]. MEGs are typically truck-mounted electricity generators, specifically designed for grid operation and support. They can be rapidly transported to areas experiencing faults and swiftly deployed. MEGs have unique advantages over their stationary counterparts. Their spatial-temporal flexibility allows for targeted provision of emergency supply, thus enhancing system resilience by functioning when stationary power solutions may fall short.

Numerous research has been undertaken to enhance power distribution network resilience using different methods. In [4], the coordination of MEGs and network reconfiguration were investigated. In scenarios of line interruptions MEG due to natural disasters, network

reconfiguration is firstly conducted by forming multiple islands, after which MEGs arrive to power the island. In [5], a rolling optimization approach is proposed to dynamically route mobile battery storage systems together with network reconfiguration. In [6], the pre-positioning and real-time dispatching of MEG were addressed and the MEG acts as a black-start generator to form microgrids to restore the critical loads. In [7], a two-stage sequential restoration method was used to schedule mobile emergency generators when distribution networks encounter extreme conditions. In [8], mobile emergency generators were used to tackle the network failure caused by hurricanes in the post-recovery stage. However, the related studies mostly focus on resilient enhancement from a network perspective and assume the network capacity is enough, which is not realistic as the electrification process continues. Meanwhile, the bottom-up flexibility sourced from local DERs is not adequately explored. Such resources, like the aggregation of roof-top solar PVs and battery energy storage systems, can support local loads to improve system resilience [9]. In [10] and [11], DER-formed microgrids were specifically utilized to improve system resilience during faults. Notably, there is also a lack of research evaluating the functionality of different flexibility resources in a coordinated manner.

To bridge this research gap, we propose a novel multi-level coordinated operation scheme to improve system resilience by combining different flexibilities. A mixed-integer linear programming (MILP) model is formulated to minimize load shedding costs and operation costs. In the event of a fault, restoration measures are sequentially conducted according to cost merits, aiming to eliminate load shedding to the most extent. Another key contribution is the integration of flexibility offered by local DERs and MEGs, and the evaluation of different flexible resources. Finally, we apply our approach to a representative European distribution network. The case study highlights the necessity of utilizing MEGs for providing emergency service with the increasing electrification rate and decreasing network capacity redundancy.

2. CONCEPTUALIZATION OF THE COORDINATED OPERATION SCHEME

Fig.1 depicts the multi-level resilient operation scheme. For future PDS, there will be various LESs with DERs. Although the LES still relies on the bulk grid, the imported electricity can be significantly reduced. For a cluster of LESs, there locates several utility-owned MEGs.

These MEG units are responsible for providing emergency services to customers when faults occur.

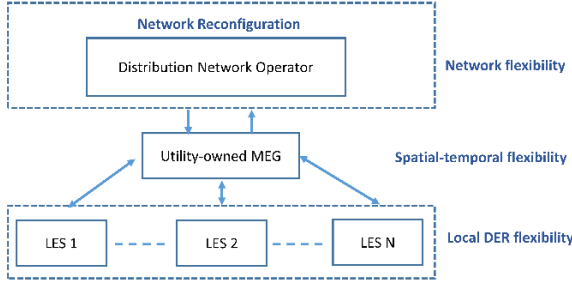


Fig. 1. Multi-level coordinated operation framework

Fig.2 illustrates the principle of how MEGs can be coordinated with other flexibility resources in a time-sequential manner. In T_1 , a fault occurs and network reconfiguration is conducted by isolating the fault and closing normally-opened switches. Meanwhile, the available DERs within the LES also support the local demand until the batteries are depleted. If the abovementioned measures cannot work, one or multiple MEGs will be transported to the fault area and then connected to the LES in T_2 to lead the role of energy supply until T_3 . In this way, all available flexibility resources can realize their potential through coordination with each other and the total load shedding amount can be reduced to the maximum extent.

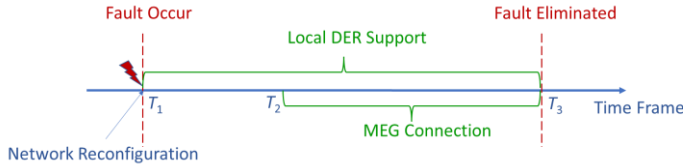


Fig. 2. Illustration of the sequential flexibilities

3. MATHEMATICAL FORMULATION OF THE PROPOSED MODEL

3.1. Objective Function

To evaluate the effectiveness of the resilient operation scheme, we formulate an optimization problem to coordinate different flexibility resources to reduce load shedding during line faults. Equation (1) illustrates the objective function, which is formulated as minimizing the total costs consisting of load shedding costs and system operation costs:

$$\begin{aligned} \min TC = & \sum_{i \in N} \sum_{t \in T} C^{VOLL} \cdot P_{i,t}^{ls} + \sum_{i \in N} \sum_{t \in T} C^{im} \cdot P_{i,t}^{im} \\ & + \sum_{k \in K} \sum_{i \in N} \sum_{t \in T} C^{trans} \cdot \mu_{k,i,t}^{trans} + \sum_{k \in K} \sum_{i \in N} \sum_{t \in T} C^{MES} \cdot P_{k,i,t}^{MES} \end{aligned} \quad (1)$$

The first term denotes the penalty costs of load shedding. The second term $C^{im} \cdot P_{i,t}^{im}$ represents the LES energy import costs from the bulk grid. The third and

fourth term denotes the costs needed for dispatching the MEG, specifically, $C^{trans} \cdot \mu_{k,i,t}^{trans}$ denotes the transportation cost due to the MEG movement, and $C^{MES} \cdot P_{k,i,t}^{MES}$ denotes the fuel cost of the MEG generation.

3.2. Network Constraints

In this research, we adopt the widely used LinDistFlow model to conduct the optimal power flow analysis [5]:

$$\sum_{(j,i) \in L} P_t^{ji} - \sum_{(j,i) \in L} P_t^{ij} = P_{i,t}^{im} - P_{i,t}^{ex}, \forall i \in N, t \in T \quad (2)$$

$$\sum_{(j,i) \in L} Q_t^{ji} - \sum_{(j,i) \in L} Q_t^{ij} = Q_{i,t}^{im} - Q_{i,t}^{ex}, \forall i \in N, t \in T \quad (3)$$

$$V_j^t - V_i^t \leq M(1 - z_{ij}) + \frac{r_{ij} P_t^{ij} + x_{ij} Q_t^{ij}}{V_0}, \forall (i, j) \in L, t \in T \quad (4)$$

$$V_j^t - V_i^t \geq -M(1 - z_{ij}) + \frac{r_{ij} P_t^{ij} + x_{ij} Q_t^{ij}}{V_0}, \forall (i, j) \in L, t \in T \quad (5)$$

$$V_i^{\min} \leq V_i^t \leq V_i^{\max}, \forall i \in N, t \in T \quad (6)$$

$$V_i^t = V_0, \forall t \in T \quad (7)$$

$$-\sqrt{2} \alpha_{ij}^t \bar{S}_{ij} \leq P_t^{ij} + Q_t^{ij} \leq \sqrt{2} \alpha_{ij}^t \bar{S}_{ij}, \forall (i, j) \in L, t \in T \quad (8)$$

$$-\sqrt{2} \alpha_{ij}^t \bar{S}_{ij} \leq P_t^{ij} - Q_t^{ij} \leq \sqrt{2} \alpha_{ij}^t \bar{S}_{ij}, \forall (i, j) \in L, t \in T \quad (9)$$

$$-\alpha_{ij}^t \bar{S}_{ij} \leq P_t^{ij} \leq \alpha_{ij}^t \bar{S}_{ij}, \forall (i, j) \in L, t \in T \quad (10)$$

$$-\alpha_{ij}^t \bar{S}_{ij} \leq Q_t^{ij} \leq \alpha_{ij}^t \bar{S}_{ij}, \forall (i, j) \in L, t \in T \quad (11)$$

In the optimization problem, network constraints are used to represent the power flow across different distribution lines. Constraints (2) and (3) model the branch power flow constraints. Specifically, $(P_{i,t}^{im} - P_{i,t}^{ex})$ and $(Q_{i,t}^{im} - Q_{i,t}^{ex})$ are the net demand of each node, indicating the energy exchange between the LES and the PDS. Constraints (4) and (5) denote the voltage drop in each branch, and the constraints are removed if the corresponding line is opened ($z_{ij} = 0$). Constraint (6) limits the voltage deviation within a defined range and the voltage is a constant value in the root bus as shown in (7). Constraints (8)-(11) models the approximate limitation of the branch capacity.

In this research, we use the spanning forest constraint to depict the network reconfiguration status. The PDS needs to keep a radial structure during operation, which corresponds to a spanning tree. After disconnecting some edges, the PDS turns from a spanning tree to multiple spanning forests. This corresponds to the case when faults occur and distribution lines are damaged. The detailed formulation of the spanning forest constraints can be found in [12]

3.3. MEG Operation Constraints

MEG can flexibly move across different locations to provide emergent supply, and there spatial-temporal behavior needs to be adequately modeled. In constraints (12)-(17), the location and function status of MEG is represented using location variables $u_{k,i,t}$ and connection variables $\lambda_{k,i,t}$. The maximum power output is limited by (12). Constraint (13) indicates that the MEG needs to reach the corresponding node first, after which it can be connected; (14) denotes the initial state of MEGs; (15) restricts that for each node, there cannot be more than one MEG connected, and (16) restricts that for a single MEG, it can only connect to one node at a time. In constraint (17), the transportation delay constraint is presented, meaning that if the MEG is in one node, it cannot reach any of the other nodes within the transportation delay.

$$0 \leq P_{k,i,t}^{MES} \leq \lambda_{k,i,t} \bar{P}_{k,i,t}^{MES}, \forall k \in K, i \in N, t \in T \quad (12)$$

$$\lambda_{k,i,t} \leq u_{k,i,t}, \forall k \in K, i \in N, t \in T \quad (13)$$

$$u_{k,i_0,t_0} = 1, \forall k \in K \quad (14)$$

$$\sum_{k \in K} \lambda_{k,i,t} \leq 1, \forall i \in N, t \in T \quad (15)$$

$$\sum_{i \in N} \lambda_{k,i,t} \leq 1, \forall k \in K, t \in T \quad (16)$$

$$u_{k,i_1,t} + u_{k,i_2,t+\tau-1} \leq 1, \forall k \in K, i_1 \neq i_2 \in N, \tau \in [1, \dots, T - T_{arr} + 1], \tau \in [1, \dots, T_{arr}] \quad (17)$$

In (18), $|u_{k,i,t+1} - u_{k,i,t}|$ indicates the change of the MEG connection state due to MEG dispatched or transported. The absolute value operator is removed by transforming (18) into (19) and (20).

$$\mu_{k,i,t} = |u_{k,i,t+1} - u_{k,i,t}|, \forall k \in K, i \in N, t \in T \setminus \{T\} \quad (18)$$

$$\mu_{k,i,t} \geq u_{k,i,t+1} - u_{k,i,t}, \forall k \in K, i \in N, t \in T \setminus \{T\} \quad (19)$$

$$\mu_{k,i,t} \geq u_{k,i,t} - u_{k,i,t+1}, \forall k \in K, i \in N, t \in T \setminus \{T\} \quad (20)$$

3.4. Load Balance Constraints

In distribution networks, local DERs are integrated with the flexibility to adjust the net import and export of the corresponding node. Constraint (21) represents the power balance constraint of each node. There exists load shedding if the demand cannot be fully met in each node, which is constrained by (22). Constraints (23) and (24) restricts that the maximum power exchange between the LES and the PDS cannot exceed the capacity limitation.

$$P_{i,t}^{im} + P_{i,t}^{pv} + P_{i,t}^{dis} + \sum_k P_{k,i,t}^{MES} = P_{i,t}^{ex} + P_{i,t}^{ch} + P_{i,t}^d \quad (21)$$

$$P_{i,t}^{ls} = P_{i,t}^D - P_{i,t}^d, \forall i \in N, t \in T \quad (22)$$

$$0 \leq P_{i,t}^{im} \leq \bar{P}_{i,t}^{im}, \forall i \in N, t \in T \quad (23)$$

$$0 \leq P_{i,t}^{ex} \leq \bar{P}_{i,t}^{ex}, \forall i \in N, t \in T \quad (24)$$

3.5. Energy Storage Constraints

Constraints (25)-(30) shows the operation of the energy storage units. Specifically, constraints (25)-(26) represents the maximum charging and discharging power; (27) limits the battery cannot be charged and discharged simultaneously. (28) represents the change of the battery state of charge in the next time step $E_{i,t+1}^{Batt}$ according to the current state of charge; and (29) limits battery state of charge within the required range. In (30), the battery remaining capacity in the end of the day is required to be the same as the initial state.

$$0 \leq P_{i,t}^{dis} \leq x_{i,t}^{dis} \bar{P}_{i,t}^{Batt}, \forall i \in N, t \in T \quad (25)$$

$$0 \leq P_{i,t}^{ch} \leq x_{i,t}^{ch} \bar{P}_{i,t}^{Batt}, \forall i \in N, t \in T \quad (26)$$

$$x_{i,t}^{ch} + x_{i,t}^{dis} \leq 1, \forall i \in N, t \in T \quad (27)$$

$$E_{i,t+1}^{Batt} = E_{i,t}^{Batt} - \frac{P_{i,t}^{dis}}{\eta} + \eta P_{i,t}^{ch}, \forall i \in N, t \in T \setminus \{T\} \quad (28)$$

$$E_{min}^{Batt} \leq E_{i,t}^{Batt} \leq E_{min}^{Batt}, \forall i \in N, t \in T \setminus \{T\} \quad (29)$$

$$E_{i,T}^{Batt} = E_{i,t_0}^{Batt}, \forall i \in N \quad (30)$$

4. CASE STUDY

In the case study, we apply the proposed coordinated operation scheme to a 20kV European representative distribution network. The network topology is shown in Fig 3, representing a semi-urban area. It features two trunk feeders from the same primary substation, interconnected via a normally-opened switch. Detailed network information is available online in [13].

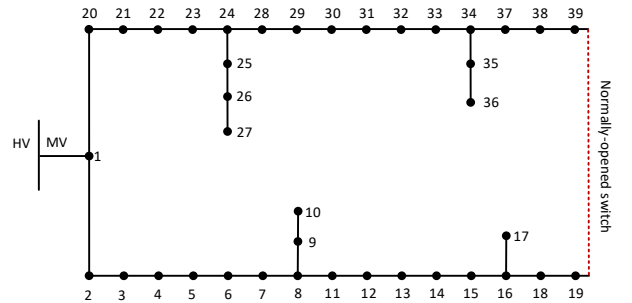


Fig. 3. European representative distribution network

Within the network area, multiple MEG units with 500kW maximum generation capacity are deployed. The related cost for driving and transporting MEG is set as £50/hour and the generation cost is £500/MWh [14]. In contrast, the value of the lost load is £25000/MWh. We assume that the MEGs can arrive at the fault area within the next hour. Each node in the network represents a LES equipped with DERs. The electricity import price is set at £200/MWh and each customer within the LESs has a

4kW rooftop PV installation, complemented by a 2kW/6kWh battery with 98% efficiency. The solar profile is generated through a geographical platform named Global Solar Atlas [15]. For load modeling, we use the residential load profile from Ofgem [16]. We consider three coordinated operation schemes in the case study:

I: Inherent network flexibility only, achieved through network reconfiguration.

II: Network flexibility coordinated with local DERs.

III: Network flexibility coordinated with local DERs and MEGs.

Additionally, we introduce two terms for specific meanings in our case study:

Local DER penetration rate: The percentage of customers equipped with DERs.

Peak demand rate: The percentage of peak demand in comparison to transformer ratings.

In this scenario, we investigate a fault that occurs on Line 1-2 and analyze the potential load shedding amount. When the peak demand percentage reaches 80%, Table I compares the three operation modes in terms of system resilient indices, such as system load shedding amount and customer average interruption duration. It is seen that network reconfiguration cannot fully eliminate load shedding, which is because the upper feeder does not have enough capacity to accommodate the transferred load.

Table I. System Resilient Indices

Operation Mode	System Total Load Shedding (MWh)	Customer Average Failure Duration (hr.)
I	10.82	1.78
II	3.58	0.59
III	0	0

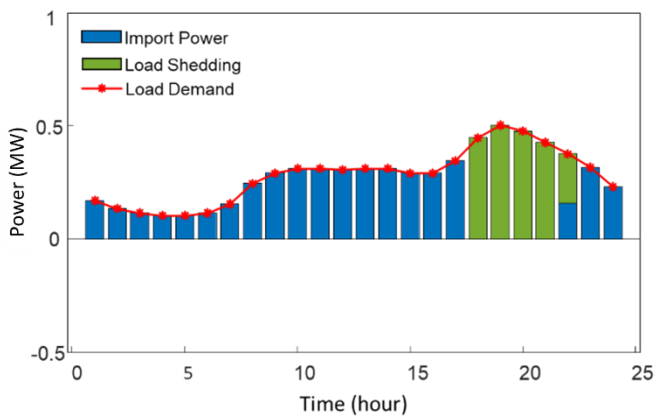


Fig. 4. System operation profile in Mode I

Fig.4 and Fig.5 display the system operation profile in different operation modes. Compared with Mode I, all

load shedding can be fully eliminated in Mode III. In the evening time, there is one MEG connected to the node near the fault line to address the peak demand that is otherwise curtailed. It is seen that the MEG not only supplies power within the LES but also exports power to support nearby loads.

Fig. 6 provides an evaluation of the variations in system load shedding amount according to the trunk feeder location and the peak demand ratio. Mode I is firstly considered to evaluate the functionality of network reconfiguration. It is shown that when the peak demand rate is below 60%, network reconfiguration as a single measure can restore most of the load effectively due to sufficient line redundancy. However, as the peak demand increases and gradually approaches transformer ratings, the system load shedding amount rises significantly.

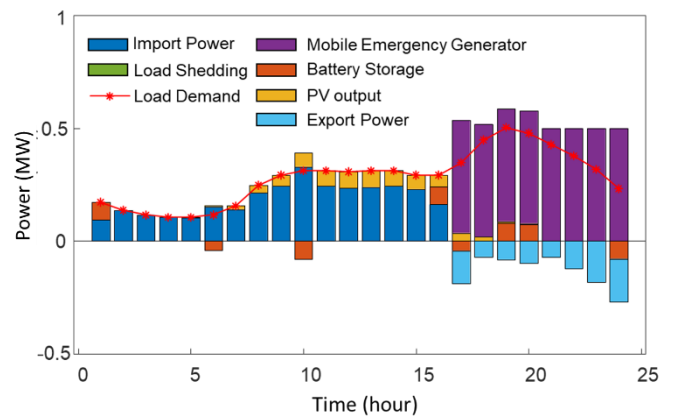


Fig. 5. System operation profile in Mode III

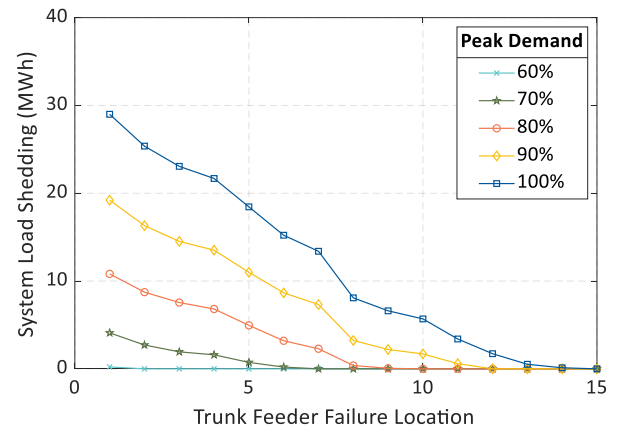


Fig. 6. System load shedding with failure locations

Fig.7 illustrates the capability of local DERs to address the increasing demand in coordination with network reconfiguration (mode II). It is seen that the increasing penetration rate of local DERs can support more load, however, when the peak demand rate exceeds 90.7%, the load shedding amount cannot be fully eliminated even if the penetration rate reaches

100%. If the load demand continues to increase, the flexibility provided by local DERs will be more limited.

In Fig.8. the performance of MEG flexibility provision in Mode III is evaluated. As the MEG capacity increases, the load shedding amount reduces initially. However, the reduction effect becomes less prominent as the capacity continues to increase, and a capacity threshold exists beyond which no further significant load shedding decrease can be observed. This is because the export power from the MEG is limited by the transformer rating. Once the transformer is fully loaded, merely increasing the MEG capacity does not result in an increased export power to supply neighboring nodes. This finding can be further extended to the case that multiple MEG units with proper capacities function better than only one single MEG unit with a larger capacity.

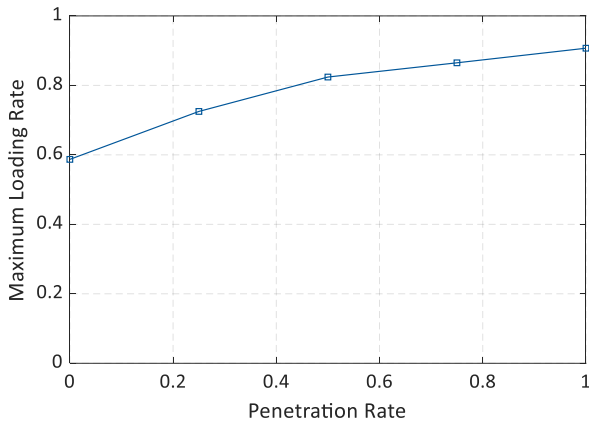


Fig. 7 Maximum loading rate and LES penetration rate

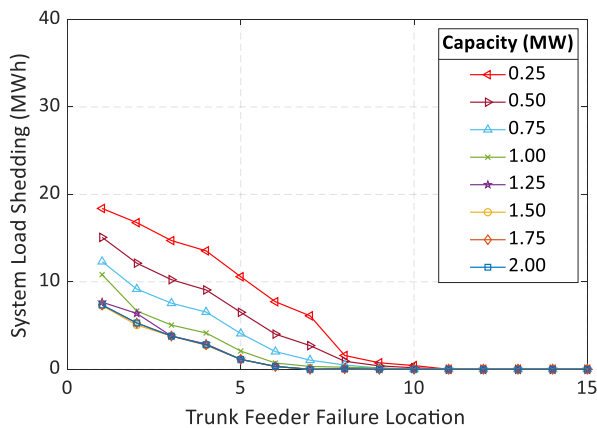


Fig. 8 System load shedding with MEG capacities

5. CONCLUSION

This paper proposes a novel coordinated operation scheme to improve the resilience of power distribution networks with increasing electrification rates. Three types of flexibility resources are investigated, including network flexibility, flexibility from local DERs, and mobile

emergency generator spatial-temporal flexibility. An optimization model to minimize system load shedding costs and operation costs is established to analyze the load shedding amount in different scenarios. We find that as network redundancy decreases, the effectiveness of network reconfiguration becomes highly restricted and may negatively impact the restoration process. Furthermore, the spatial-temporal flexibility offered by mobile emergency generators demonstrates unique effectiveness in improving system resilience by coordinating with networks and DERs.

ACKNOWLEDGEMENT

This work is supported by the China Scholarship Council, the EPSRC UK/China MC2 project (EP/T021969/1) and the Supergen Energy Networks Hub Project (EP/S00078X/2).

DECLARATION OF INTEREST STATEMENT

The authors declare that they have no known competing financial interests or personal relationships that could have appeared to influence the work reported in this paper. All authors read and approved the final manuscript.

REFERENCE

- [1] R. Jing, Y. Zhou, and J. Wu. "Electrification with flexibility towards local energy decarbonization." *Advances in Applied Energy* 5 (2022): 100088.
- [2] Y. Zhou, J. Wu. (2021, Jul.). Peer-to-peer energy trading in microgrids and local energy systems, N. Jenkins, Ed. London, United Kingdom: IntechOpen, 2021.
- [3] M. Yuan, et al. "Optimal planning of mobile emergency generators of resilient distribution system." *Energy Reports* 8 (2022): 1404-1413.
- [4] G. Zhang, et al. "Mobile emergency generator planning in resilient distribution systems: A three-stage stochastic model with non-anticipativity constraints." *IEEE Transactions on Smart Grid* 11.6 (2020): 4847-4859.
- [5] X. Liu, H. Zhang, and T. Zhao, "Rolling optimization of mobile energy storage fleets for resilient service restoration," *IEEE Transactions on Smart Grid* 11.2 (2019): 1030-1043
- [6] S. Lei, J. Wang, C. Chen, and Y. Hou, "Mobile Emergency Generator Pre-Positioning and Real-Time Allocation for Resilient Response to Natural Disasters," *IEEE Transactions on Smart Grid* 9.3 (2016): 2030-2041.
- [7] C., Sheng, Y. Xie, Q. Wu, X. Jin, M. Zhang, and Z. Xiang. "Two-stage mobile emergency generator dispatch for sequential service restoration of microgrids in extreme

conditions." International Journal of Electrical Power & Energy Systems 153 (2023): 109312.

[8] A. Kavousi-Fard, M. Wang and W. Su, "Stochastic Resilient Post-Hurricane Power System Recovery Based on Mobile Emergency Resources and Reconfigurable Networked Microgrids," IEEE Access 6 (2018): 72311-72326.

[9] E. Galvan, P. Mandal, and Y. Sang, "Networked microgrids with roof-top solar PV and battery energy storage to improve distribution grids resilience to natural disasters," International Journal of Electrical Power & Energy Systems 123 (2020): 106239.

[10] H., Akhtar, V. Bui, and H. Kim. "Microgrids as a resilience resource and strategies used by microgrids for enhancing resilience." Applied energy 240 (2019): 56-72.

[11] C. Chen, J. Wang, F. Qiu, and D. Zhao, "Resilient distribution system by microgrids formation after natural disasters," IEEE Transactions on smart grid 7.2 (2015): 958-966.

[12] S. Lei, C. Chen, Y. Song, and Y. Hou, "Radiality constraints for resilient reconfiguration of distribution systems: Formulation and application to microgrid formation," IEEE Transactions on Smart Grid 11.5 (2020): 3944-3956

[13] "Distribution System Operators Observatory", JRC Smart Electricity Systems and Interoperability, 2020. [Online]

Available at: <https://ses.jrc.ec.europa.eu/distribution-system-operators-observatory>. (Accessed 15 Oct. 2023)

[14] S., Hedayat, and S. Jadid. "Mobile and self-powered battery energy storage system in distribution networks—Modeling, operation optimization, and comparison with stationary counterpart." Journal of Energy Storage 42 (2021): 103068.

[15] "Global Solar Atlas Platform. [Online]. Available at: <https://globalsolaratlas.info/map>. (Accessed 15 Oct. 2023).

[16] "Energy Demand Research Project (EDRP)," Ofgem. [Online] Available: <https://www.ofgem.gov.uk/energy-policy-and-regulation/policy-and-regulatory-programmes/energy-demand-research-project-edrp>. (Accessed 15 Oct. 2023)